Assessing Climate Change Impacts on Live Fuel Moisture and Wildfire Risk Using a Hydrodynamic Vegetation Model

Wu Ma[1], Lu Zhai[2], Alexandria Pivovaroff[3], Jacquelyn Shuman[4], Polly Buotte[5], Junyan Ding[6], Bradley Christoffersen[7], Ryan Knox[6], Max Moritz[8], Rosie A. Fisher[9], Charles D. Koven[6], Lara Kueppers[10], Chonggang Xu[1,]*

[1]Earth and Environmental Sciences Division, Los Alamos National Laboratory, Los Alamos, NM, United States

[2]Department of Natural Resource Ecology and Management, Oklahoma State University, Stillwater, OK, United States

[3]Atmospheric Science and Global Change Division, Pacific Northwest National Laboratory, Richland, WA, United States

[4]National Center for Atmospheric Research, Climate and Global Dynamics, Terrestrial Sciences Section, Boulder, CO, United States

[5]Energy and Resources Group, University of California, Berkeley, CA, United States

[6]Climate and Ecosystem Sciences Division, Lawrence Berkeley National Laboratory, CA, United States

[7]Department of Biology, University of Texas Rio Grande Valley, Edinburg, TX, United States

[8]UC ANR Cooperative Extension, Bren School of Environmental Science & Management, University of California, Santa Barbara, CA, United States

[9]Centre Européen de Recherche et de Formation Avancée en Calcul Scientifique, Toulouse, France

[10]Energy and Resources Group, University of California, Berkeley, and Lawrence Berkeley National Laboratory, Berkeley, CA, United States

25   *Corresponding author (Chonggang Xu, cxu@lanl.gov)*

26   **Abstract:** Live fuel moisture content (LFMC) plays a critical role in wildfire dynamics, but little

27   is known about responses of LFMC to multivariate climate change, e.g., warming temperature,

28   CO_2 fertilization and altered precipitation patterns, leading to a limited prediction ability of

29   future wildfire risks. Here, we use a hydrodynamic demographic vegetation model to estimate

30   LFMC dynamics of chaparral shrubs, a dominant vegetation type in fire-prone southern

31   California. We parameterize the model based on observed shrub allometry and hydraulic traits,

32   and evaluate the model's accuracy through comparisons between observed and simulated LFMC

33   of three plant functional types (PFTs) under current climate conditions. Moreover, we estimate

34   the number of days per year of LFMC below 79% (which is a critical threshold for wildfire

35   danger rating of southern California chaparral shrubs) from 1960 to 2099 for each PFT, and

36   compare the number of days below the threshold for medium and high greenhouse gas emission

37   scenarios (RCP4.5 and 8.5). We find that climate change could lead to more days per year (5.2-

38   14.8% increase) with LFMC below 79% between the historical (1960-1999) and future (2080-

39   2099) periods, implying an increase in wildfire danger for chaparral shrubs in southern

40   California. Under the high greenhouse gas emission scenario during the dry season, we find that

41   the future LFMC reductions mainly result from a warming temperature, which leads to 9.1-

42   18.6% reduction in LFMC. Lower precipitation in the spring leads to a 6.3-8.1% reduction in

43   LFMC. The combined impacts of warming and precipitation change on fire season length are

44   equal to the additive impacts of warming and precipitation change individually. Our results show

45   that the CO_2 fertilization will mitigate fire risk by causing a 3.5-4.8% increase in LFMC. Our

46   results suggest that multivariate climate change could cause a significant net reduction in LFMC

47   and thus exacerbate future wildfire danger in chaparral shrub systems.

48   **Keywords:** FATES-HYDRO, chaparral shrubs, plant functional types, southern California, CO_2

49   enrichment, climate change

1. Introduction

51   Historical warming and changes in precipitation have already impacted wildfire at a

52   global scale (e.g. Stocks et al. 1998; Gillett et al. 2004; Westerling et al. 2003, 2006) and it is

53   expected that accelerating future warming will continue to significantly influence global wildfire

54   regimes (e.g. Flannigan et al. 2009; Liu et al. 2010; Moritz et al. 2012). So far, prior studies have

55   mainly focused on impacts of dead fuel moisture, fuel loads, and weather conditions on wildfire.

56   Limited studies have applied proxies of live fuel moisture in global-fire models. For example,

57   dead fuel moisture is found to be related to fire ignition and fire spread potential (or potential

58   area burnt) (Aguado et al. 2007), specific weather conditions such as increased vapor pressure

59   deficit (Williams et al. 2019) can lead to a vast increase in fire activity (Goss et al. 2020), and

60   wildfire fuel loads are projected to increase under climate change (Matthews et al. 2012; Clarke

61   et al. 2016). In global-fire models, studies have used proxies of live fuel moisture (Bistinas et al.

62   2014; Kelley et al. 2019) as well as explicit representation of live fuels (Hantson et al. 2016;

63   Rabin et al. 2017). While previous studies provide great insights into fire risks with changes in

64   climate, dead fuel moisture, fuel loads, and representation of live fuel moisture, there is still

65   limited understanding of how climate change influences live fuel moisture content (LFMC) and

66   the consequent wildfire risks. This is particularly true for the combined impacts of warming

67   temperature, altered precipitation, and increasing CO_2 fertilization (Chuvieco et al. 2004;

68   Pellizzaro 2007; Caccamo et al. 2012a, b; Williams et al. 2019; Goss et al. 2020).

69   A measure of water content within living plant tissue in relation to their dry weight,

70   LFMC has been found to be one of the most critical factors influencing combustion, fire spread,

71   and fire consumption (e.g. Agee et al. 2002; Zarco-Tejada et al. 2003; Bilgili & Saglam 2003;

72   Yebra et al. 2008; Dennison et al. 2008; Anderson & Anderson 2010; Keeley et al. 2011). This is

73   because a low LFMC leads to increased flammability and a higher likelihood of ignition

74   (Dimitrakopoulos & Papaioannou 2001). For instance, LFMC was found to be a significant

75   factor contributing to the occurrence of wildfires in Australia (Plucinski 2003; Nolan et al. 2016;

76   Yebra et al. 2018; Rossa & Fernandes 2018; Pimont et al. 2019), Spain (Chuvieco et al. 2009)

77   and California (Santa Monica Mountains; Dennison et al. 2008; Dennison & Moritz 2009;

78   Pivovaroff et al. 2019). Dennison & Moritz (2009) found strong evidence of a LFMC threshold

79   (79%) for southern California chaparral shrubs, which may determine when large fires can occur

80   in this region.

81   Vegetation moisture content is dependent on both ecophysiological characteristics of the

82   species and environmental conditions, including both climatic variables and soil water

83   availability (Rothermel 1972; Castro et al. 2003; Castro et al. 2003; Pellizzaro 2007; Pivovaroff

84   et al. 2019; Nolan et al. 2020). So far, little is known about the relative importance of different

85   climate variables to future LFMC dynamics. On the one hand, warming could contribute to a

86   higher atmospheric demand and higher evapotranspiration (Rind et al. 1990) and thus lead to a

87   lower LFMC. On the other hand, higher CO_2 concentration will decrease stomatal conductance

88   (Wullschleger et al. 2002) and plant water loss, and thus lead to a higher LFMC. The impacts of

89   CO_2 and warming could be complicated by local changes in precipitation patterns and humidity

90   (Mikkelsen et al. 2008).

91   The sensitivity of LFMC to climate change is likely to be affected by plant hydraulic

92   traits (the plant properties that regulate water transport and storage within plant tissues), which

93   affect plant water regulation (Wu et al. 2020). Variations in hydraulic traits reflect contrasting

94   plant drought adaptation strategies when responding to dry conditions. Two contrasting overall

95   strategies are: 1) water stress avoiders and 2) water stress tolerators (Tobin et al. 1999; Wei et al.

96   2019). The "avoiders" are generally characterized by a more conservative hydraulic strategy

97   under water stress by either closing stomata early, dropping leaves or accessing deep water to

98   avoid more negative water potentials and therefore xylem cavitation. Meanwhile, the "tolerators"

99   typically build xylem and leaves that are more resistant to cavitation so that they can tolerate

100 more negative water potential and continue to conduct photosynthesis under water stress.

101 Therefore, compared with the tolerators, the avoiders normally have a lower sapwood density

102 and higher plant water storage capacity in their tissues to avoid cavitation (Meinzer et al. 2003,

103 2009; Pineda-Garcia et al. 2013). Because the avoiders rely on water storage capacity as one way

104 to avoid cavitation thereby maintaining a relatively high LFMC, and water loss from storage

105 should increase with warming, LFMC could be more sensitive to climate change in avoiders

106 relative to tolerators.

107   While over half of terrestrial landscapes on Earth are considered fire-prone (Krawchuk et

108 al. 2009), Mediterranean-type climate regions are routinely impacted by fire, often on an annual

109 basis. This is partly because Mediterranean climate regions are characterized by winter rains

110 followed by annual dry season, when little to no rainfall occurs for several months. Multiday

111 periods of extreme high temperatures, as well as katabatic hot, dry, and intense winds, often

112 punctuate the annual drought, leading to some of the worst fire weather in the world (Schroeder

113 et al. 1964). This can result in wildfires that are large, high-intensity, and stand-replacing

114 (Keeley 1995; Keeley & Zedler 2009; Balch et al. 2017). Globally, Mediterranean climate

115 regions are characterized by evergreen sclerophyllous-leaved shrublands. The Mediterranean

116 climate region in California is dominated by chaparral, which is adapted to the periodic fire

117   regime in California (Venturas et al. 2016). Previous studies have proposed a variety of

118   relationships between chaparral LFMC and fire danger in southern California (Dennison et al.

119   2008; Dennison & Moritz 2009), but less is known about how climate changes could alter LFMC

120   and fire danger. In chaparral, LFMC is usually high during the winter and spring (wet season)

121   and then gradually declines during the dry season (summer and fall), which leads to a typical fire

122   season approximately six months long in southern California (Pivovaroff et al. 2019). One key

123   risk is that severe drought conditions are becoming exacerbated under climate change, which

124   might lead to the occurrence of larger and higher-intensity fires in chaparral (Dennison et al.

125   2008; Dennison & Moritz 2009).

126   There has been a long history of wildfire modeling, with three types of models: 1) fine-

127   scale fire behavior models (e.g. FIRETEC by Linn et al. 2002); 2) landscape-scale fire

128   disturbance models (e.g. LANDIS-II by Sturtevant et al. 2009); and 3) global-scale fire dynamics

129   models (e.g. Hantson et al. 2016; Rabin et al. 2017; SPITFIRE by Thonicke et al. 2010). While

130   these models focus on simulation at different scales, fire measures of the simulation are mainly

131   calculated from climate and dead fuel moisture and currently lack prediction of LFMC dynamics.

132   One key limitation is that most previous models have not yet considered plant hydrodynamics

133   (Holm et al. 2012; Xu et al. 2013; Seiler et al. 2014), which is integral to LFMC prediction.

134   Recently, there have been important improvements to global dynamic and demographic

135   vegetation models by incorporating plant hydrodynamics (McDowell et al. 2013; Xu et al. 2016;

136   Fisher et al. 2018; Mencuccini et al. 2019). These models have been used to study the interaction

137   between elevated CO_2 and drought (Duursma & Medlyn, 2012), the impact of hydraulic traits on

138   plant drought response (Christofferson et al. 2016), the role of hydraulic diversity in vegetation

139   response to drought (Xu et al. 2016) and hydroclimate change (Powell et al. 2018), and

140 vegetation water stress and root water uptake (Kennedy et al. 2019). While the main purpose of

141 the new hydraulic components is to improve the vegetation response to drought, the fact that

142 hydrodynamic models consider tissue water content as a prognostic variable provides an

143 opportunity to assess the climate impacts on LFMC.

144   The objective of this study is to quantify LFMC dynamics and associated changes in fire

145 season duration for a chaparral ecosystem in southern California under climate change using a

146 vegetation demographic model (that resolves the size and age-since-disturbance structure of

147 plant populations) (Xu et al. 2016; Fisher et al. 2018) that incorporates plant hydraulics. We test

148 one overarching hypothesis: future climate change will decrease LFMC and consequently result

149 in a longer fire season as determined by a critical threshold of LFMC (H_0). Specifically, we test

150 the following four sub-hypotheses: 1) warming has a stronger impact on LFMC than CO_2

151 fertilization (H_1); 2) the reductions in spring and autumn precipitation lead to a longer fire season

152 as determined by LFMC (H_2); 3) the combined impacts of warming and precipitation on fire

153 season length are equal to the additive impacts of warming and precipitation change individually

154 (H_3); and 4) LFMC for plants with more conservative hydraulic strategies ("avoiders") will be

155 more vulnerable to warming (H_4).

2. Materials and Methods

157   To understand climate change impacts on LFMC for the chaparral ecosystem, we applied

158 the Functionally Assembled Terrestrial Simulator (FATES; Fisher et al. 2015; Massoud et al.

159 2019; Koven et al. 2020) coupled with a hydrodynamic vegetation module (FATES-HYDRO;

160 Christoffersen et al. 2016) in the Santa Monica Mountains in California. We validated the model

161 using the observed LFMC for three chaparral shrub plant functional types (PFTs). Then, we

162 applied FATES-HYDRO to estimate long-term dynamics of leaf water content (LWC) during

163   1960-2099 for each PFT using downscaled Earth System Model (ESM) climate scenarios. We

164   converted simulated leaf water content (LWC) to LFMC within leaves and shoots. Based on the

165   simulated LFMC, we evaluated wildfire danger based on the number of days per year of LFMC

166   below the critical value of 79% from 1960 to 2099 for each PFT under RCP 4.5 and 8.5. Finally,

167   we assessed the relative importance of changes in individual and combined climate variables

168   including CO_2, temperature, precipitation, ~~and relative humidity~~ and tested the corresponding

169   hypotheses.

2.1 Study site

171   The study site is located at the Stunt Ranch Santa Monica Mountains Reserve, in the

172   Santa Monica Mountains in California, USA (N 34° 05', W 118° 39'). Stunt Ranch is dominated

173   by chaparral vegetation, with an elevation of approximately 350 m, a west-facing slope, and a

174   Mediterranean-type climate. The study site harbors an abundance of fauna, particularly birds and

175   reptiles. The mean annual temperature is 18.1°C. The mean annual precipitation is 478 mm,

176   occurring mostly during the wet season (i.e. November-March) with almost no rainfall during the

177   dry season (i.e. April-October). Stunt Ranch last burned in year 1993 ~~but has recovered well~~. We

178   focused on PFTs representing 11 study species (Fig. 1), including chamise (*Adenostoma*

179   *fasciculatum* - Af), red shank (*Adenostoma sparsifolium* - As), big berry manzanita

180   (*Arctostaphylos glauca* - Ag), buck brush (*Ceanothus cuneatus* - Cc), greenbark ceanothus

181   (*Ceanothus spinosus* - Cs), mountain mahogany (*Cercocarpus betuloides* - Cb), toyon

182   (*Heteromeles arbutifolia* - Ha), laurel sumac (*Malosma laurina* - Ml), scrub oak (*Quercus*

183   *berberidifolia* - Qb), hollyleaf redberry (*Rhamnus ilicifolia* - Ri), and sugar bush (*Rhus ovata* -

184   Ro). Detailed information about the study site and species characterizations found at Stunt Ranch

185   can be found in Venturas et al. (2016) and Pivovaroff et al. (2019).

2.2 FATES-HYDRO model

FATES is a vegetation demographic model (Fisher et al. 2015), which uses a size-structured group of plants (cohorts) and successional trajectory-based patches based on the ecosystem demography approach (Moorcroft et al. 2001). FATES simulates the demographic process including seed production, seed emergence, growth and mortality (Koven et al. 2020). Because the main purpose is to assess LFMC, we controlled for variation in plant size structure that could arise from plant traits or climate differences between model runs by using a reduced-complexity configuration of the model where growth and mortality are turned off and ecosystem structure is held constant. FATES has to be hosted by a land surface model to simulate the soil hydrology, canopy temperature and transpiration. These host land models include the Exascale Energy Earth System Model (E3SM, Caldwell et al., 2019) land model (ELM) as well as the Community Earth System Model (Fisher et al 2015) and the Norwegian Earth system model (NorESM, Tjiputra et al 2013). In this study, we used the DOE-sponsored ELM as our host land model. The time step of FATES to calculate carbon and water fluxes is 30 minutes and it can downscale the data from 6-hourly climate drivers.

A key component of FATES, the plant hydrodynamic model (HYDRO, based on Christoffersen et al. 2016), simulates the water flow from soil through root, stem and leaf to the atmosphere. In this model, water flow is calculated based on water pressure gradients across different plant compartments (leaf, stem, transporting roots, absorbing roots and rhizosphere). Specifically, flow between compartment i and $i + 1$ (Q_i) is given by

$$Q_i = -K_i \Delta h_i, \tag{1}$$

where K_i is the total conductance (kg MPa^{-1} s^{-1}) at the boundary of compartments i and $i + 1$ and Δh_i is the total water potential difference between the compartments:

$$\Delta h_i = \rho_w g(z_i - z_{i+1}) + (\psi_i - \psi_{i+1}), \tag{2}$$

208   where z_i is compartment distance above (+) or below (-) the soil surface (m), ρ_w is the density of

209   water (10^3 kg m^{-3}), g is acceleration due to gravity (9.8 m s^{-2}), and ψ_i is tissue or soil matric

210   water potential (MPa). K_i is treated here as the product of a maximum boundary conductance

211   between compartments i and $i + 1$ ($K_{max,i}$), and the fractional maximum hydraulic conductance

212   of the adjacent compartments (FMC_i or FMC_{i+1}), which is a function of the tissue water content.

213   A key parameter that controls FMC is the critical water potential (P$_{50}$) that leads to 50% loss of

214   hydraulic conductivity. The tissue water potential is calculated based on pressure-volume (PV)

215   theory (Tyree & Hammel, 1972; Tyree & Yang, 1990; Bartlett et al., 2012). For leaves, it is

216   described by three phases: 1) capillary water phase with full turgor, 2) elastic drainage phase

217   before reaching turgor loss point; and 3) post-turgor loss phase. For other tissues, it only has

218   phases 2 and 3. Compared to a non-hydrodynamic model, this formulation allows the simulation

219   of plant water transport limitation on transpiration. For the non-hydrodynamic version of

220   FATES, the water limitation factor for transpiration (B$_{tran}$) is calculated based on the soil

221   moisture potential (Fisher et al. 2015). For the hydrodynamic version, B$_{tran}$ is calculated based on

222   the leaf water potential (ψ_l) (Christoffersen et al. 2016) as follows,

$$B_{tran} = [1 + (\frac{\psi_l}{P_{50\_gs}})^{a_l}]^{-1} \tag{3}$$

224   where P_{50_gs} is the leaf water potential that leads to 50% loss of stomatal conductance and a_l is

225   the shape parameter. Please refer to Christoffersen, et al. 2016 for details of formulations of

226   FMC for different plant tissues.

227   **2.3 Allometry and trait data for model parameterization**

228   FATES-HYDRO has a large number of parameters (>80; see Massoud et al. 2019 for a

229   complete list except for hydraulic parameters). Based on a previous sensitivity analysis study

230   (Massoud et al. 2019), we focused our parameter estimation efforts on the most influential

231   parameters for allometry, leaf and wood traits, and hydraulic traits from observations of 11

232   chaparral shrub species (see Supplementary, Table S2), collected from Jacobsen et al. (2008) and

233   Venturas et al. (2016). For this study, we assumed that the allometry of a shrub is analogous to

234   that of a small tree. However, we did make several important modifications to accommodate the

235   allometry of shrub as their height and crown area relationships to diameter could be different

236   from trees. First, instead of using the diameter at breast height as the basis for allometry to

237   calculate the height, crown area and leaf biomass, we used the basal diameter as the basis for

238   shrubs. Second, in the allometry of trees, the diameter for maximum height (d_1:

239   Fates_allom_dbh_maxheight, Table S1) is the same as the diameter for maximum crown area (d_2:

240   Fates_allom_d2ca_max, Table S1). As our data showed that d_1 and d_2 are different for shrubs,

241   we have modified the codes so that the d_1 and d_2 can be set for different values. It is possible that

242   different branching and path length patterns for stems of chaparral species could impact the

243   hydraulics compared to trees; however, FATES-HYDRO treats all the aboveground xylem as a

244   single pool and thus it should not affect our model simulation results.

245   Based on a hierarchical cluster analysis (Bridges 1966) of allometry and trait data, there

246   are a clear separation among the shrub species. First, the dendrogram is built and every data

247   point finally merges into a single cluster with the height shown on the y-axis. Then we cut the

248   dendrogram in order to create the desired number of clusters determined by a pragmatic choice

249   based on hydraulic traits of eleven chaparral shrub species (Fig. 1). R's rect.hclust function

250   (https://www.rdocumentation.org/packages/stats/versions/3.6.2/topics/rect.hclust) was used to

251 see the clusters on the dendrogram. All parameters of allometry, leaf and wood traits, and

252 hydraulic traits were collected from observations shown in the Table S2 and S3 of the

253 supplementary. According to the principle of model parsimony, we do not want to classify the

254 species into more than 3 PFTs. Meanwhile, we also want to differentiate the fundamental plant

255 growth and water use strategies that will determine plant transpiration rate and the corresponding

256 LFMC. If we choose to classify the species into two PFTs (based on the solid horizontal line in

257 Fig. 1), then we will not be able to differentiate species with aggressive and conservative

258 hydraulic strategies in the second group and not be able to test H4. Therefore, the chaparral

259 shrub species were classified into three PFTs (based on the dotted horizontal line in Fig. 1 and

260 Table S3), that are able to differentiate plant growth and hydraulic strategy. The three PFTs

261 include a low productivity, aggressive drought tolerance hydraulic strategy PFT (PFT-LA) with a

262 relative low $V_{c,max25}$ (the maximum carboxylation rate at 25 °C) and a very negative P_{50} (the leaf

263 water potential leading to 50% loss of hydraulic conductivity); a medium productivity,

264 conservative drought tolerance hydraulic strategy PFT (PFT-MC) represented by a medium

265 $V_{c,max25}$ and a less negative P_{50}, turgor loss point and water potential at full turgor; and a high

266 productivity, aggressive drought tolerance hydraulic strategy PFT (PFT-HA) with a relatively

267 high $V_{c,max25}$ and a very negative P_{50}. The mean of species-level trait data weighted by species

268 abundance at the site were used to parameterize FATES-HYDRO.

269 **2.4 Model initialization**

270   Our model simulation is transient in terms of soil water content, leaf water content,

271 carbon and water fluxes. The forest structure (plant sizes and number density) is fixed and is

272 parameterized based on a vegetation inventory from Venturas et al. (2016). The soil texture and

273 depth information are parameterization based on a national soil survey database

274   (https://websoilsurvey.sc.egov.usda.gov/App/WebSoilSurvey.aspx; Table S1). The soil moisture

275   is initialized with 50% of the saturation and the tissue plant water content is initialized so that it

276   is in equilibrium with the soil water potential. We run the model for 10 years based on 1950-

277   1960 climate so that the simulated soil moisture, leaf water content, carbon and water fluxes are

278   not depending on their initial conditions.

2.5 Live Fuel Moisture Content for model validation

280   In this study, we used measured LFMC to validate simulated LFMC. FATES-HYDRO

281   does not directly simulate the LFMC. Thus, we estimated the LFMC based on simulated LWC.

282   The LWC in the model is calculated as follows,

283     $$\text{LWC} = \frac{fw - dw}{dw} * 100, \tag{4}$$

284   where, *fw* is the fresh weight and *dw* is the dry weight, which are simulated within FATES-

285   HYDRO. Then, we estimated the LFMC within leaves and shoots (< 6 mm diameter) using the

286   empirical equation derived from shrub LFMC and LWC data including the three regenerative

287   strategies [seeder (S), resprouter (R) and seeder–resprouter (SR)], in summer, autumn and winter

288   from Fig. 4 and 5 in Saura-Mas and Lloret's study (2007) as follows (Fig. S4),

289     $$\text{LFMC} = 31.091 + 0.491\text{LWC}, \tag{5}$$

290   The climate in Saura-Mas and Lloret's study is Mediterranean (north-east Iberian Peninsula),

291   which is consistent with the climate of our study area. LFMC was measured on our site

292   approximately every three weeks, concurrently with plant water potentials in 2015 and 2016.

293   LFMC measurement details can be found in Pivovaroff et al. (2019). For comparison with our

294   model outputs, we calculated the mean LFMC within leaves and shoots for each PFT weighted

295 by the species abundance (Venturas et al. 2016). Species abundance was calculated by dividing

296 mean density of a specific species by the mean density of all species.

2.6 Climate drivers

298 We forced the FATES-HYDRO model with 6-hourly temperature, ~~relative humidity,~~

299 precipitation, downward solar radiation, and wind components. Historical climate data during

300 2012-2019, which were used for FATES-HYDRO calibration, were extracted from a local

301 weather station (https://stuntranch.ucnrs.org/weather-date/). Historical and future climate data

302 during 1950-2099, which were used for simulations of LFMC by FATES-HYDRO model, were

303 downloaded from the Multivariate Adaptive Constructed Analogs (MACA) datasets (Abatzoglou

304 & Brown 2012; http://maca.northwestknowledge.net). The MACA datasets (1/24-degree or

305 approximately 4-km; Abatzoglou & Brown 2012) include 20 ESMs with historical forcings

306 during 1950-2005 and future Representative Concentration Pathways (RCPs) RCP 4.5 and

307 RCP8.5 scenarios during 2006-2099 from the native resolution of the ESMs. The gridded surface

308 meteorological dataset METDATA (Abatzoglou, 2013) were used with high spatial resolution

309 (1/24-degree) and daily timescales for near-surface minimum/maximum temperature,

310 ~~minimum/maximum relative humidity,~~ precipitation, downward solar radiation, and wind

311 components. Then we downscaled the MACA daily data to 6-hourly based on the temporal

312 anomaly of the observed mean daily data to the hourly data for each day during 2012-2019. The

313 model is driven by yearly CO_2 data obtained from Meinshausen et al (2011).

2.7 Hypothesis testing

315 To test H_0 (future climate change will decrease LFMC and consequently result in a longer

316 fire season as determined by a critical threshold of LFMC), we compared the simulated mean

317   LFMC, derived from modeled leaf water content, under the climate projections from 20 ESMs

318   under RCP 4.5 and 8.5. We then tested if the LFMC during the April-October dry season in the

319   historic period of 1960-1999 is significantly higher than that in the future period of 2080-2099.

320   For the fire season duration, we estimated the number of days per year below a critical threshold

321   of LFMC (79%). Similarly, we tested if the number of days per year below the critical threshold

322   of LFMC during the historical period are significantly different from that during the future

323   period. We used a bootstrapped approach (Jackson 1993) to test if the mean of LFMC or fire

324   season duration are significantly different between these two periods. Specifically, we randomly

325   draw 10000 samples from the simulated residuals of LFMCs or fire season durations estimated

326   by 20 ESMs for these two periods under the null hypothesis that there is no difference in the

327   mean. We then calculated p-values by comparing the simulated mean difference to the empirical

328   distribution of difference estimated from these 10000 samples. See Supplementary section 5.2

329   within Xu et al. (2019) for the details.

330   To test H_1 (warming has a stronger impact on LFMC than CO_2 fertilization), we

331   compared mean simulated LFMC and fire season length for three PFTs with/without CO_2

332   changes (fixed CO_2 at 367 ppm vs dynamic CO_2 concentrations from RCP 4.5 or RCP 8.5) and

333   warming. To remove the future warming trend, future temperature was replaced with historical

334   (1986-2005) temperature data for every 20 year period. Similarly, to test H_2 (the reductions in

335   spring and autumn precipitation lead to a longer fire season as determined by LFMC), we

336   compared the model outputs of LFMC and fire season length for three PFTs with/without

337   precipitation changes. To test H_3 (the combined impacts of warming and precipitation on fire

338   season length are equal to the additive impacts of warming and precipitation change

339   individually), we compared model outputs of LFMC and fire season length for three PFTs under

340   three scenarios: 1) without warming; 2) without precipitation changes; and 3) without warming

341   and precipitation changes. Finally, to test H4 (LFMC for plants with more conservative hydraulic

342   strategies will be more vulnerable to warming), we compared model outputs of LFMC and fire

343   season length across the three different PFTs with different hydraulic strategies.

3. Results

3.1 Comparison between simulated and measured LFMC

346   Our results showed that FATES-HYDRO was able to capture variation in the LFMC for

347   different PFTs and soil water content in 5-cm depth (Fig. 2 and S3), also for Chamise in 2018

348   (Fig. S5) although we had limited observed LFMC data. Specifically, the model was able to

349   capture 96%, 86%, and 80% of the variance in observed LFMC for the period of 2015-2016 for

350   three PFTs, respectively (Fig. 2 b, d, f). The model was also able to capture the seasonal

351   dynamics of soil water content, LFMC, and LFMC below the threshold 79% in comparison to

352   observed data (Fig. 2 a, c, e and S3). To validate that FATES-HYDRO is able to capture the

353   interannual variability of LFMC, we compared the simulated LFMC for PFT-LA with the long-

354   term observations of LFMC for the chamise species (*Adenostoma fasiculatum*; Fig. S5). Our

355   results showed that the model is able to reasonably capture the seasonal and interannual

356   variability for the period of 2006-2019 (R^2=0.7), although it underestimates peaks in LFMC in 4

357   of 14 years.

3.2 Changes in the LFMC and fire season length from historical to future periods

359   Using the validated model driven by climate projections from 20 ESMs under greenhouse

360   gas emission scenarios RCP4.5 and RCP 8.5, we found that the daily mean LFMC during the

361   future period of 2080-2099 was projected to become significantly lower than that during the

362 historical period of 1960-1999 for all three PFTs (Fig 3, P<0.000001). Our results also showed

363 that the spread among models increase with time, suggesting a larger uncertainty in the

364 projection into the future. Specifically, the histogram of daily mean LFMC during the April-

365 October dry season showed that there was a higher probability of low LFMC under future

366 climate conditions (Fig. S1). The daily mean LFMC decreased from 84.7%, 101.3%, and 78.4%

367 during the historical period of 1960-1999 to 81.0-82.8%, 96.3-98.8%, and 74.8-76.6% during the

368 future period of 2080-2099 under both climate scenarios for PFT-LA, PFT-MC, PFT-HA,

369 respectively (Fig 3).

370   Based on the projected LFMC, there was a significant increase in the fire season length

371 with the critical threshold of LFMC from the historical period of 1960-1999 to the future period

372 of 2080-2099 for three PFTs. With the critical threshold of 79% LFMC, the fire season length

373 was projected to increase by 20, 22, 19 days under RCP 8.5 (Fig. 4 and Table S4), and to

374 increase by 9, 11, 8 days under RCP 4.5 (Fig. 4 and Table S4). Our results also showed that the

375 spread among models increase with time, suggesting a larger uncertainty in the projection into

376 the future. The above results for mean LFMC and fire season length support hypothesis H_0 that

377 future climate change will decrease LFMC and consequently result in a longer fire season, as

378 determined by critical thresholds for LFMC, for all three PFTs.

379 **3.3 Relative effects of individual climate changes on the length of the fire season**

380   In order to better understand the relative contribution to fire season length of different

381 climate variables, we ran FATES-HYDRO for three PFTs using meteorological forcings that

382 isolated and removed changes in individual specific variables. Our results showed that the

383 increase in fire season length mainly resulted from warming, which led to 16-23 days (9.1-

384 18.6%) per year increase in fire season length for the critical threshold of 79% LFMC under RCP

385   8.5 (Fig. 5). This is because warming is pushing Vapor Pressure Deficit (VPD) higher, resulting

386   in increased fire season length. For RCP 4.5, the warming contributed to 5-6 days (3.8-4.3%) per

387   year increase in fire season length (Fig. 5). We also found that elevated CO_2 concentrations

388   decreased fire season length with 6-7 days (3.5-4.8%) per year decrease in fire season length

389   under RCP 8.5 (Fig. 5). Under RCP 4.5, CO_2 increases led to 2-3 days (1.5-2.2%) per year

390   decrease in fire season length (Fig. 5). Because the impact of warming on fire season length was

391   stronger than the mitigation from CO_2 enrichment, our results support hypothesis H_1 (warming

392   has a stronger impact on LFMC than CO_2 fertilization).

393   Even though total precipitation was projected to increase in the future, lower precipitation

394   in the spring and autumn (Fig. S2 a, b) led to 8-10 days (6.3-8.1%) per year increase in fire

395   season length with the critical threshold of 79% LFMC under RCP 8.5 (Fig. 5). Under RCP 4.5,

396   the precipitation changes contributed to 1-3 days (0.8-1.6%) increase in fire season length (Fig.

397   5). This result supported hypothesis H_2 that the reductions in spring and autumn precipitation

398   lead to a longer fire season as determined by LFMC.

399   Our results showed that the combined impacts of warming and precipitation on fire

400   season length were equal to the additive impacts of warming and precipitation change

401   individually. This supported hypothesis H_3. Specifically, the combined changes in temperature

402   and precipitation caused 24-33 days per year (15.6-26.8%) increase in fire season length with the

403   critical threshold of 79% LFMC under RCP 8.5 (Fig. 5). Under RCP 4.5, the combined changes

404   in temperature and precipitation caused a 6-9 days per year (4.8-6.1%) change in fire season

405   length.

406   **3.4 Comparison of changes in fire season length among three PFTs under climate change**

407   Regarding three PFTs under both climate scenarios, fire season length of PFT-HA was

408   the longest (167-176 days per year), while fire season length of PFT-MC was the shortest (114-

409   124 per year) during 2080-2099 (Fig. 4). However, the response of fire season length to warming

410   was strongest for PFT-MC. Specifically, for PFT-MC, warming under RCP 8.5 led to an increase

411   of 21.6% (22 days) in fire season length (Fig. 5 b) and warming under RCP 4.5 led to an increase

412   of 10.8% (11 days) in fire season length. For PFT-LA, warming under RCP 8.5 led to an increase

413   of 14.7% (19 days) in fire season length (Fig. 5 a) while warming under RCP 4.5 led to an

414   increase of 7.4% (9 days) in fire season length. Finally, for PFT-HA, warming under RCP 8.5 led

415   to an increase of 10.2% (18 days) in fire season length (Fig. 5 c) and 5.3% (8 days) in fire season

416   length with under RCP 4.5. Because PFT-MC has a more conservative hydraulic strategy with

417   less negative P_{50}, turgor loss point and water potential at full turgor, this result supported

418   hypothesis H_4 that the LFMC for plants with more conservative hydraulic strategy will be more

419   vulnerable to warming.

420   To validate our classification scheme, we compared these PFT-level results to those

421   obtained with single-PFT and 2-PFT simulations finding that using the three PFTs defined by our

422   cluster analysis gives a qualitatively different view of LFMC change than a single- or 2-PFT

423   simulation. We found significant differences in the percentage changes of LFMC and fire season

424   length between future period (2080-2099) and historical period (1960-1999) using three distinct

425   PFTs, but no significant differences between PFTs in 2-PFT simulations under the different

426   climate scenarios (Fig. S6).

427   **4. Discussion**

428   Low LFMC within shrub leaves and shoots increases the flammability and likelihood of

429   combustion, making it vitally important to monitor temporal variations in LFMC, especially

430 during the dry season (Dennison et al, 2008). The strong relationships between observed and

431 simulated LFMC of all PFTs (Fig. 2) suggested that the plant hydrodynamic model, FATES-

432 HYDRO, could accurately estimate LFMC seasonal dynamics as a function of modeled leaf

433 water content, and consequently be useful to predict fire risks in Mediterranean-type climate

434 regions, although only small amount of validation data were used and the underlying assumption

435 that a shrub was analogous to a small tree. Based on the simulated monthly mean LFMC during

436 2006-2019 for PFT-LA, which includes the chamise species, we found that our model can

437 capture the seasonal variation and interannual variability, but underestimates the highest wet

438 season peaks in LFMC in 4 of 14 years (Fig. S5). This may cause biases for future projections

439 while it would not highly affect the long-term trend of LFMC and fire season length. During the

440 future period (2080-2099) and the historical period (1960-1999), both periods displayed lower

441 values in the dry season (April - October), which is consistent with lower LFMC during the

442 summer-fall dry season, rather than the winter-spring wet season (Chuvieco et al, 2004;

443 Pellizzaro et al, 2007; Pivovaroff et al. 2019). Extremely low daily LFMC was more likely to

444 occur during the future period, which had higher temperature than the historical period. From the

445 historical to the future period, fire season length could increase by 5.2-14.8% under climate

446 change for chaparral shrub ecosystems (H_0). The fire season length was not validated, rather it

447 was defined as number of days with LFMC below 79%.

448   Quantifying influences of climatic variables on LFMC is crucial to predicting future fire

449 risks (Dennison & Moritz, 2009). Our results showed that future warming was the most

450 important driver of LFMC while relative humidity was the least important driver. This finding

451 suggested that warming would substantially push Vapor Pressure Deficit (VPD) higher and

452 decrease LFMC and strongly increase the fire season length, which may greatly increase fire

453 risks in the future (e.g. Dennison et al, 2008; Chuvieco et al, 2009; Pimont et al, 2019). ~~Relative~~

454 ~~humidity would not strongly affect LFMC under climate change.~~ CO_2 fertilization is expected to

455 reduce stomatal conductance (Pataki et al. 2000; Tognetti et al. 2000) and thus could mitigate the

456 impacts of warming on LFMC. Our results illustrated that, even though the CO_2 impact did cause

457 a 3.5-4.8% reduction in fire season length, the impact of warming on fire season length is about

458 5.6-13.8% larger than the CO_2 effect (H_1, warming has a stronger impact on LFMC than CO_2

459 fertilization). This result suggests that CO_2 fertilization cannot offset the LFMC impacts from

460 warming. The FATES-HYDRO model assumes a consistent stomatal sensitivity to CO_2

461 concentration across Mediterranean shrub species. While Mediterranean shrub functional types

462 in arid and semi-arid systems would vary in their stomatal response in the real world (Pataki et

463 al. 2000). Therefore, our model may overestimate/underestimate the CO_2 effect on stomatal

464 conductance and its mitigating influence might be smaller in reality for some species.

465   Previous studies implied that the timing of precipitation may have a strong impact on

466 subsequent LFMC (e.g. Veblen et al. 2000; Westerling et al. 2006; Dennison & Moritz 2009). In

467 this study, precipitation was also a key driver of LFMC under future climate conditions. Our

468 results showed that, even though total precipitation was projected to increase, the reduction in

469 spring and autumn precipitation (Fig. S2) was projected to cause a longer fire season length (H_2,

470 the reductions in spring and autumn precipitation lead to a longer fire season as determined by

471 LFMC; Fig. 5). This result was in agreement with a prior study indicating that spring

472 precipitation, particularly in the month of March, was found to be the primary driver of timing of

473 LFMC changes (Dennison & Moritz 2009). We also found that the combined impacts of

474 warming and precipitation on fire season length were equal to the linearly additive impacts of

475 warming and precipitation change individually (H_3). Our results suggested that, when evaluating

476 future fire risks, it is critical that we considered the seasonal changes in precipitation and its

477 interaction with the warming impact.

478   Modeled vegetation responses to environmental changes is a function of variation in plant

479 functional traits (Koven et al, 2020). The three PFTs represented in this study have similar

480 patterns in LFMC in response to climate change during 1960-2099, but we did see some critical

481 differences. Specifically, the plant functional type PFT-MC with more conservative hydraulic

482 strategy had the strongest responses to climate change (Fig. 5). This could be related to the fact

483 that the PFT-MC is a more conservative drought tolerant PFT in terms of hydraulic strategy with

484 less negative P_{50}, turgor loss point, and water potential at full turgor. The PFT-MC plants had a

485 relatively high saturated water content based on observed data (Fig 2) and the water within plant

486 tissues thus changes more quickly in response to the environmental condition changes (H4, ~~plants~~

487 LFMC for plants with more conservative hydraulic strategies will be more vulnerable to

488 warming). However, the three different PFTs were coexisting at the same location in model

489 simulations, coexistence and heterogeneity in LFMC might impact fire behavior and fire season

490 length.

491   Because the moisture content of live fuels (~50–200%) are much higher than that of dead

492 fuels (~7–30%), leaf senescence induced by drought stress and subsequent mortality are

493 potentially vital factors to cause large wildfires (Nolan et al. 2016, 2020). Thus drought-induced

494 canopy die-back and mortality could largely increase surface fine fuel loads and vegetation

495 flammability, which can increase the probability of wildfire (Ruthrof et al. 2016). Since growth

496 and mortality are turned off in model runs by using a reduced-complexity configuration, it is

497 possible that vegetation density might decrease and LFMC could be conserved under future

498 scenarios. In addition, potential vegetation transitions (e.g., shrubs to grassland and species

499 composition changes) might substantially affect flammability and thus fire intensity and

500 frequency. In this study, we used the static mode of FATES-HYDRO to simulate LWC dynamics

501 under climate change. If we need to assess how the leaf senescence and vegetation dynamics will

502 impact the fire behavior, we can use the same model with dynamic mode to assess their impacts

503 on fire behaviors under future drought and warming conditions.

504 Application of a hydrodynamic vegetation model to estimate LFMC dynamics could

505 potentially benefit wildfire modeling at the fine-scale, landscape-scale, and global-scale. This is

506 because LFMC is one of the most critical factors influencing combustion, fire spread, and fire

507 consumption while previous wildfire models mainly focus on impacts of dead fuel moisture,

508 weather conditions on wildfire, fuel loads, and representation of live fuel moisture (Anderson &

509 Anderson 2010; Keeley et al. 2011; Jolly & Johnson 2018). The implications of this are that fire

510 potential will vary with plant water potential and uptake from soils, photosynthetic and

511 respiratory activity, carbon allocation and phenology with variability across species and over

512 time (Jolly & Johnson 2018). Therefore, future work to incorporate LFMC dynamics in wildfire

513 models could potentially play a vitally important role in the future studies of wildfire modeling

514 under climate change.

515 **5. Conclusions**

516 A hydrodynamic vegetation model, FATES-HYDRO, was used to estimate leaf water

517 status and thus LFMC dynamics of chaparral shrub species in southern California under

518 historical and future conditions. FATES-HYDRO model was validated using monthly mean

519 LFMC for three PFTs. The fire season length was projected to substantially increase under both

520 climate scenarios from 1960-1999 to 2080-2099. This could increase wildlife risk over time for

521 chaparral shrubs in southern California. Our results showed that temperature was the most

important driver of LFMC ~~and relative humidity was the least important~~ among ~~four~~ all climatic

variables ~~including CO_2, temperature, precipitation, and relative humidity~~. The LFMC estimated

by the FATES-HYDRO model offered a baseline of predicting plant hydraulic dynamics

subjected to climate change and provided a critical foundation that reductions in LFMC from

climate warming may exacerbate future wildfire risk. Longer fire season might have a significant

impact on overall public health and quality of life in the future.

Acknowledgements

This project is supported by the University of California Office of the President Lab Fees

Research Program and the Next Generation Ecosystem Experiment (NGEE) Tropics, which is

supported by the U.S. DOE Office of Science. CDK and JD are supported by the DOE Office of

Science, Regional and Global Model Analysis Program, Early Career Research Program. R

statistical software is applied to make figures for this study. A repository link for FATES is

https://github.com/xuchongang/fates.

References

Abatzoglou, J.T. and Brown, T.J., 2012. A comparison of statistical downscaling methods suited

for wildfire applications. *International Journal of Climatology*, *32*(5), pp.772-780.

Abatzoglou JT (2013) Development of gridded surface meteorological data for ecological

applications and modelling. *International Journal of Climatology*, 33, 121-131.Agee, J.K.,

Wright, C.S., Williamson, N. and Huff, M.H., 2002. Foliar moisture content of Pacific Northwest

vegetation and its relation to wildland fire behavior. *Forest ecology and management*, *167*(1-3),

pp.57-66.

543 Anderson, S.A. and Anderson, W.R., 2010. Ignition and fire spread thresholds in gorse (Ulex

544 europaeus). *International Journal of Wildland Fire*, *19*(5), pp.589-598.

545 Aguado, I., Chuvieco, E., Boren, R. and Nieto, H., 2007. Estimation of dead fuel moisture

546 content from meteorological data in Mediterranean areas. Applications in fire danger assessment.

547 *International Journal of Wildland Fire*, *16*(4), pp.390-397.

548 Bistinas, I., Harrison, S.P., Prentice, I.C. and Pereira, J.M.C., 2014. Causal relationships versus

549 emergent patterns in the global controls of fire frequency. *Biogeosciences*, *11*(18), pp.5087-5101.

550 Burgan, R.E. Estimating Live Fuel Moisture for the 1978 National Fire Danger Rating System;

551 Intermountain Forest and Range Experiment Station: Ogden, UT, USA, 1979.

552 Bilgili, E. and Saglam, B., 2003. Fire behavior in maquis fuels in Turkey. *Forest Ecology and

553 Management*, *184*(1-3), pp.201-207.

554 Balch, J.K., Bradley, B.A., Abatzoglou, J.T., Nagy, R.C., Fusco, E.J. and Mahood, A.L., 2017.

555 Human-started wildfires expand the fire niche across the United States. *Proceedings of the

556 National Academy of Sciences*, *114*(11), pp.2946-2951.

557 Bartlett, M.K., Scoffoni, C. and Sack, L., 2012. The determinants of leaf turgor loss point and

558 prediction of drought tolerance of species and biomes: a global meta-analysis. *Ecology letters*,

559 *15*(5), pp.393-405.

560 Bridges Jr, C.C., 1966. Hierarchical cluster analysis. *Psychological reports*, *18*(3), pp.851-854.

561 Christoffersen, B.O., Gloor, M., Fauset, S., Fyllas, N.M., Galbraith, D.R., Baker, T.R., Kruijt, B.,

562 Rowland, L., Fisher, R.A., Binks, O.J. and Sevanto, S., 2016. Linking hydraulic traits to tropical

forest function in a size-structured and trait-driven model (TFS v. 1-Hydro). Geoscientific Model

Development. 9: 4227-4255.

Caccamo, G., Chisholm, L.A., Bradstock, R.A. and Puotinen, M.L., 2012a. Using remotely-

sensed fuel connectivity patterns as a tool for fire danger monitoring. *Geophysical Research*

Letters, *39*(1).

Caccamo, G., Chisholm, L.A., Bradstock, R.A., Puotinen, M.L. and Pippen, B.G., 2012b.

Monitoring live fuel moisture content of heathland, shrubland and sclerophyll forest in south-

eastern Australia using MODIS data. *International Journal of Wildland Fire*, *21*(3), pp.257-269.

Clarke, H., Pitman, A.J., Kala, J., Carouge, C., Haverd, V. and Evans, J.P., 2016. An

investigation of future fuel load and fire weather in Australia. *Climatic Change*, *139*(3-4),

pp.591-605.

Chuvieco, E., Cocero, D., Riano, D., Martin, P., Martınez-Vega, J., de la Riva, J. and Pérez, F.,

2004. Combining NDVI and surface temperature for the estimation of live fuel moisture content

in forest fire danger rating. Remote Sensing of Environment, 92(3), pp.322-331.

Caldwell, P.M., Mametjanov, A., Tang, Q., Van Roekel, L.P., Golaz, J.C., Lin, W., Bader, D.C.,

Keen, N.D., Feng, Y., Jacob, R. and Maltrud, M.E., 2019. The DOE E3SM coupled model

version 1: Description and results at high resolution. *Journal of Advances in Modeling Earth*

Systems, *11*(12), pp.4095-4146.

Castro, F.X., Tudela, A. and Sebastià, M.T., 2003. Modeling moisture content in shrubs to

predict fire risk in Catalonia (Spain). *Agricultural and Forest Meteorology*, *116*(1-2), pp.49-59.

583 Chuvieco, E., González, I., Verdú, F., Aguado, I. and Yebra, M., 2009. Prediction of fire

584 occurrence from live fuel moisture content measurements in a Mediterranean ecosystem.

585 *International Journal of Wildland Fire*, *18*(4), pp.430-441.

586 Collins, M., Knutti, R., Arblaster, J., Dufresne, J.L., Fichefet, T., Friedlingstein, P., Gao, X.,

587 Gutowski, W.J., Johns, T., Krinner, G. and Shongwe, M., 2013. Long-term climate change:

588 projections, commitments and irreversibility. In *Climate Change 2013-The Physical Science*

589 *Basis: Contribution of Working Group I to the Fifth Assessment Report of the Intergovernmental*

590 *Panel on Climate Change* (pp. 1029-1136). Cambridge University Press.

591 Cook, B.I., Smerdon, J.E., Seager, R. and Coats, S., 2014. Global warming and 21 st century

592 drying. *Climate Dynamics*, *43*(9-10), pp.2607-2627.

593 Dennison, P.E., Moritz, M.A. and Taylor, R.S., 2008. Evaluating predictive models of critical

594 live fuel moisture in the Santa Monica Mountains, California. *International Journal of Wildland*

595 *Fire*, *17*(1), pp.18-27.

596 Dennison, P.E. and Moritz, M.A., 2009. Critical live fuel moisture in chaparral ecosystems: a

597 threshold for fire activity and its relationship to antecedent precipitation. *International Journal of*

598 *Wildland Fire*, *18*(8), pp.1021-1027.

599 Dimitrakopoulos, A.P. and Papaioannou, K.K., 2001. Flammability assessment of Mediterranean

600 forest fuels. *Fire Technology*, *37*(2), pp.143-152.

601 Dai, A., 2013. Increasing drought under global warming in observations and models. *Nature*

602 *climate change*, *3*(1), pp.52-58.

603 Duursma, R.A. and Medlyn, B.E., 2012. MAESPA: a model to study interactions between water

604 limitation, environmental drivers and vegetation function at tree and stand levels, with an

605 example application to $[CO_2] \times$ drought interactions.

606 Flannigan, M.D., Krawchuk, M.A., de Groot, W.J., Wotton, B.M. and Gowman, L.M., 2009.

607 Implications of changing climate for global wildland fire. *International journal of wildland fire*,

608 *18*(5), pp.483-507.

609 Fisher, R.A., Williams, M., Da Costa, A.L., Malhi, Y., Da Costa, R.F., Almeida, S. and Meir, P.,

610 2007. The response of an Eastern Amazonian rain forest to drought stress: results and modelling

611 analyses from a throughfall exclusion experiment. *Global Change Biology*, *13*(11), pp.2361-

612 2378.

613 Fisher, R.A., Muszala, S., Verteinstein, M., Lawrence, P., Xu, C., McDowell, N.G., Knox, R.G.,

614 Koven, C., Holm, J., Rogers, B.M. and Spessa, A., 2015. Taking off the training wheels: the

615 properties of a dynamic vegetation model without climate envelopes, CLM4. 5 (ED).

616 *Geoscientific Model Development*, *8*(11), pp.3593-3619.

617 Fisher, R.A., Koven, C.D., Anderegg, W.R., Christoffersen, B.O., Dietze, M.C., Farrior, C.E.,

618 Holm, J.A., Hurtt, G.C., Knox, R.G., Lawrence, P.J. and Lichstein, J.W., 2018. Vegetation

619 demographics in Earth System Models: A review of progress and priorities. *Global change*

620 *biology*, *24*(1), pp.35-54.

621 Gillett, N.P., Weaver, A.J., Zwiers, F.W. and Flannigan, M.D., 2004. Detecting the effect of

622 climate change on Canadian forest fires. *Geophysical Research Letters*, *31*(18).

623   Goss, M., Swain, D.L., Abatzoglou, J.T., Sarhadi, A., Kolden, C.A., Williams, A.P. and

624   Diffenbaugh, N.S., 2020. Climate change is increasing the likelihood of extreme autumn wildfire

625   conditions across California. *Environmental Research Letters*, *15*(9), p.094016.

626   Hantson, S., Arneth, A., Harrison, S.P., Kelley, D.I., Prentice, I.C., Rabin, S.S., Archibald, S.,

627   Mouillot, F., Arnold, S.R., Artaxo, P. and Bachelet, D., 2016. The status and challenge of global

628   fire modelling. *Biogeosciences*, *13*(11), pp.3359-3375.

629   Holm, J.A., Shugart, H.H., Van Bloem, S.J. and Larocque, G.R., 2012. Gap model development,

630   validation, and application to succession of secondary subtropical dry forests of Puerto Rico.

631   *Ecological Modelling*, *233*, pp.70-82.

632   Jacobsen, A. L., Pratt, R. B., Davis, S. D., & Ewers, F. W. (2008). Comparative community

633   physiology: nonconvergence in water relations among three semi-arid shrub communities. New

634   Phytologist, 180(1), 100-113.

635   Jolly, W.M. and Johnson, D.M., 2018. Pyro-ecophysiology: shifting the paradigm of live

636   wildland fuel research. *Fire*, *1*(1), p.8.

637   Jackson, D.A., 1993. Stopping rules in principal components analysis: a comparison of

638   heuristical and statistical approaches. *Ecology*, *74*(8), pp.2204-2214.

639   Kelley, D.I., Bistinas, I., Whitley, R., Burton, C., Marthews, T.R. and Dong, N., 2019. How

640   contemporary bioclimatic and human controls change global fire regimes. *Nature Climate*

641   *Change*, *9*(9), pp.690-696.

642 Konings, A.G., Rao, K. and Steele-Dunne, S.C., 2019. Macro to micro: microwave remote

643 sensing of plant water content for physiology and ecology. *New Phytologist*, *223*(3), pp.1166-

644 1172.

645 Keeley, J.E., 1995. Future of California floristics and systematics: wildfire threats to the

646 California flora. Madrono, pp.175-179.

647 Keeley, J.E. and Zedler, P.H., 2009. Large, high-intensity fire events in southern California

648 shrublands: debunking the fine-grain age patch model. *Ecological Applications*, *19*(1), pp.69-94.

649 Keeley, J.E., Bond, W.J., Bradstock, R.A., Pausas, J.G. and Rundel, P.W., 2011. *Fire in*

650 *Mediterranean ecosystems: ecology, evolution and management*. Cambridge University Press.

651 Kennedy, D., Swenson, S., Oleson, K.W., Lawrence, D.M., Fisher, R., Lola da Costa, A.C. and

652 Gentine, P., 2019. Implementing plant hydraulics in the community land model, version 5.

653 *Journal of Advances in Modeling Earth Systems*, *11*(2), pp.485-513.

654 Koven, C.D., Knox, R.G., Fisher, R.A., Chambers, J.Q., Christoffersen, B.O., Davies, S.J.,

655 Detto, M., Dietze, M.C., Faybishenko, B., Holm, J. and Huang, M., 2020. Benchmarking and

656 parameter sensitivity of physiological and vegetation dynamics using the Functionally

657 Assembled Terrestrial Ecosystem Simulator (FATES) at Barro Colorado Island, Panama.

658 *Biogeosciences*, *17*(11), pp.3017-3044.

659 Krawchuk, M.A., Moritz, M.A., Parisien, M.A., Van Dorn, J. and Hayhoe, K., 2009. Global

660 pyrogeography: the current and future distribution of wildfire. *PloS one*, *4*(4), p.e5102.Linn, R.,

661 Reisner, J., Colman, J.J. and Winterkamp, J., 2002. Studying wildfire behavior using FIRETEC.

662 *International journal of wildland fire*, *11*(4), pp.233-246.

663   Liu, Y., Stanturf, J. and Goodrick, S., 2010. Trends in global wildfire potential in a changing

664   climate. *Forest ecology and management*, *259*(4), pp.685-697.

665   Massoud, E.C., Xu, C., Fisher, R.A., Knox, R.G., Walker, A.P., Serbin, S.P., Christoffersen,

666   B.O., Holm, J.A., Kueppers, L.M., Ricciuto, D.M. and Wei, L., 2019. Identification of key

667   parameters controlling demographically structured vegetation dynamics in a land surface model:

668   CLM4. 5 (FATES). *Geoscientific Model Development*, *12*(9), pp.4133-4164.

669   Moorcroft, P.R., Hurtt, G.C. and Pacala, S.W., 2001. A method for scaling vegetation dynamics:

670   the ecosystem demography model (ED). *Ecological monographs*, *71*(4), pp.557-586.

671   Mikkelsen, T.N., Beier, C., Jonasson, S., Holmstrup, M., Schmidt, I.K., Ambus, P., Pilegaard,

672   K., Michelsen, A., Albert, K., Andresen, L.C. and Arndal, M.F., 2008. Experimental design of

673   multifactor climate change experiments with elevated CO_2, warming and drought: the

674   CLIMAITE project. *Functional Ecology*, *22*(1), pp.185-195.

675   Moritz, M.A., Parisien, M.A., Batllori, E., Krawchuk, M.A., Van Dorn, J., Ganz, D.J. and

676   Hayhoe, K., 2012. Climate change and disruptions to global fire activity. *Ecosphere*, *3*(6), pp.1-

677   22.

678   McDowell, N.G., Fisher, R.A., Xu, C., Domec, J.C., Hölttä, T., Mackay, D.S., Sperry, J.S.,

679   Boutz, A., Dickman, L., Gehres, N. and Limousin, J.M., 2013. Evaluating theories of drought-

680   induced vegetation mortality using a multimodel–experiment framework. *New Phytologist*,

681   *200*(2), pp.304-321.

682   Mencuccini, M., Manzoni, S. and Christoffersen, B., 2019. Modelling water fluxes in plants:

683   from tissues to biosphere. *New Phytologist*, *222*(3), pp.1207-1222.

684   Matthews, S., Sullivan, A.L., Watson, P. and Williams, R.J., 2012. Climate change, fuel and fire

685   behaviour in a eucalypt forest. *Global Change Biology*, *18*(10), pp.3212-3223.

686   Manabe, S. and Wetherald, R.T., 1975. The effects of doubling the CO2 concentration on the

687   climate of a general circulation model. *Journal of the Atmospheric Sciences*, *32*(1), pp.3-15.

688   Meinzer, F.C., James, S.A., Goldstein, G. and Woodruff, D., 2003. Whole-tree water transport

689   scales with sapwood capacitance in tropical forest canopy trees. *Plant, Cell & Environment*,

690   *26*(7), pp.1147-1155.

691   Meinzer, F.C., Johnson, D.M., Lachenbruch, B., McCulloh, K.A. and Woodruff, D.R., 2009.

692   Xylem hydraulic safety margins in woody plants: coordination of stomatal control of xylem

693   tension with hydraulic capacitance. *Functional Ecology*, *23*(5), pp.922-930.

694   Meinshausen, M., Smith, S.J., Calvin, K., Daniel, J.S., Kainuma, M.L., Lamarque, J.F.,

695   Matsumoto, K., Montzka, S.A., Raper, S.C., Riahi, K. and Thomson, A.G.J.M.V., 2011. The

696   RCP greenhouse gas concentrations and their extensions from 1765 to 2300. *Climatic change*,

697   *109*(1), pp.213-241.

698   Nolan, R.H., Boer, M.M., Resco de Dios, V., Caccamo, G. and Bradstock, R.A., 2016. Large-

699   scale, dynamic transformations in fuel moisture drive wildfire activity across southeastern

700   Australia. *Geophysical Research Letters*, *43*(9), pp.4229-4238.

701   Nolan, R.H., Blackman, C.J., de Dios, V.R., Choat, B., Medlyn, B.E., Li, X., Bradstock, R.A.

702   and Boer, M.M., 2020. Linking forest flammability and plant vulnerability to drought. *Forests*,

703   *11*(7), p.779.

704 National Fuel Moisture Database. 2021.

705 https://www.wfas.net/nfmd/public/site.php?site_fuel=Stunt%20Road%2C%20Calabasas&gacc=

706 SOCC&state=CA&grup=LA%20County&sitefuel=site&display_type=Table%20Only%20Actua

707 l%20Data&fuel_selected=Chamise.

708 Pivovaroff, A. L., Emery, N., Sharifi, M. R., Witter, M., Keeley, J. E., & Rundel, P. W. (2019).

709 The effect of ecophysiological traits on live fuel moisture content. Fire, 2(2), 28.

710 Powell, T.L., Koven, C.D., Johnson, D.J., Faybishenko, B., Fisher, R.A., Knox, R.G., McDowell,

711 N.G., Condit, R., Hubbell, S.P., Wright, S.J. and Chambers, J.Q., 2018. Variation in

712 hydroclimate sustains tropical forest biomass and promotes functional diversity. *New*

713 *Phytologist*, *219*(3), pp.932-946.

714 Pellizzaro, G., Cesaraccio, C., Duce, P., Ventura, A. and Zara, P., 2007. Relationships between

715 seasonal patterns of live fuel moisture and meteorological drought indices for Mediterranean

716 shrubland species. *International Journal of Wildland Fire*, *16*(2), pp.232-241.

717 Plucinski, M.P., 2003. The investigation of factors governing ignition and development of fires

718 in heathland vegetation. *PhD thesis. University of New South Wales, Sydney.*

719 Pimont, F., Ruffault, J., Martin-StPaul, N.K. and Dupuy, J.L., 2019. Why is the effect of live fuel

720 moisture content on fire rate of spread underestimated in field experiments in shrublands?.

721 *International journal of wildland fire*, *28*(2), pp.127-137.

722 Pataki, D.E., Huxman, T.E., Jordan, D.N., Zitzer, S.F., Coleman, J.S., Smith, S.D., Nowak, R.S.

723 and Seemann, J.R., 2000. Water use of two Mojave Desert shrubs under elevated CO2. *Global*

724 *Change Biology*, *6*(8), pp.889-897.

725   Pineda-Garcia, F., Paz, H. and Meinzer, F.C., 2013. Drought resistance in early and late

726   secondary successional species from a tropical dry forest: the interplay between xylem resistance

727   to embolism, sapwood water storage and leaf shedding. *Plant, Cell & Environment*, *36*(2),

728   pp.405-418.

729   Rabin, S.S., Melton, J.R., Lasslop, G., Bachelet, D., Forrest, M., Hantson, S., Kaplan, J.O., Li,

730   F., Mangeon, S., Ward, D.S. and Yue, C., 2017. The Fire Modeling Intercomparison Project

731   (FireMIP), phase 1: experimental and analytical protocols with detailed model descriptions.

732   *Geoscientific Model Development*, *10*(3), pp.1175-1197.

733   Rossa, C.G. and Fernandes, P.M., 2018. Live fuel moisture content: The 'pea under the mattress'

734   of fire spread rate modeling?. *Fire*, *1*(3), p.43.

735   Rind, D., Goldberg, R., Hansen, J., Rosenzweig, C. and Ruedy, R., 1990. Potential

736   evapotranspiration and the likelihood of future drought. *Journal of Geophysical Research:*

737   *Atmospheres*, *95*(D7), pp.9983-10004.

738   Rothermel, R.C., 1972. *A mathematical model for predicting fire spread in wildland fuels* (Vol.

739   115). Intermountain Forest & Range Experiment Station, Forest Service, US Department of

740   Agriculture.

741   Ruthrof, K.X., Fontaine, J.B., Matusick, G., Breshears, D.D., Law, D.J., Powell, S. and Hardy,

742   G., 2016. How drought-induced forest die-off alters microclimate and increases fuel loadings and

743   fire potentials. *International Journal of Wildland Fire*, *25*(8), pp.819-830.

744   Sturtevant, B.R., Scheller, R.M., Miranda, B.R., Shinneman, D. and Syphard, A., 2009.

745   Simulating dynamic and mixed-severity fire regimes: a process-based fire extension for

746   LANDIS-II. *Ecological Modelling*, *220*(23), pp.3380-3393.

747 Stocks, B.J., Fosberg, M.A., Lynham, T.J., Mearns, L., Wotton, B.M., Yang, Q., Jin, J.Z.,

748 Lawrence, K., Hartley, G.R., Mason, J.A. and McKenney, D.W., 1998. Climate change and

749 forest fire potential in Russian and Canadian boreal forests. *Climatic change*, *38*(1), pp.1-13.

750 Schroeder, M.J., Glovinsky, M., Henricks, V.F., Hood, F.C. and Hull, M.K., 1964. *Synoptic*

751 *weather types associated with critical fire weather*. USDA Forest Service, Pacific Southwest

752 Range and Experiment Station. Berkeley, CA.

753 Seiler, C., Hutjes, R.W.A., Kruijt, B., Quispe, J., Añez, S., Arora, V.K., Melton, J.R., Hickler, T.

754 and Kabat, P., 2014. Modeling forest dynamics along climate gradients in Bolivia. *Journal of*

755 *Geophysical Research: Biogeosciences*, *119*(5), pp.758-775.

756 Sheffield, J. and Wood, E.F., 2008. Projected changes in drought occurrence under future global

757 warming from multi-model, multi-scenario, IPCC AR4 simulations. *Climate dynamics*, *31*(1),

758 pp.79-105.

759 Saura-Mas, S. and Lloret, F., 2007. Leaf and shoot water content and leaf dry matter content of

760 Mediterranean woody species with different post-fire regenerative strategies. *Annals of Botany*,

761 *99*(3), pp.545-554.

762 Sun, W., Maseyk, K., Lett, C. and Seibt, U., 2016. Litter dominates surface fluxes of carbonyl

763 sulfide in a Californian oak woodland. *Journal of Geophysical Research: Biogeosciences*,

764 *121*(2), pp.438-450.

765 Thonicke, K., Spessa, A., Prentice, I.C., Harrison, S.P., Dong, L. and Carmona-Moreno, C.,

766 2010. The influence of vegetation, fire spread and fire behaviour on biomass burning and trace

767 gas emissions: results from a process-based model. *Biogeosciences*, *7*(6), pp.1991-2011.

768   Tyree, M.T. and Hammel, H.T., 1972. The measurement of the turgor pressure and the water

769   relations of plants by the pressure-bomb technique. *Journal of experimental Botany*, *23*(1),

770   pp.267-282.

771   Tyree, M.T. and Yang, S., 1990. Water-storage capacity of Thuja, Tsuga and Acer stems

772   measured by dehydration isotherms. *Planta*, *182*(3), pp.420-426.

773   Tognetti, R., Minnocci, A., Peñuelas, J., Raschi, A. and Jones, M.B., 2000. Comparative field

774   water relations of three Mediterranean shrub species co-occurring at a natural CO2 vent. *Journal*

775   *of Experimental Botany*, *51*(347), pp.1135-1146.

776   Tjiputra, J.F., Roelandt, C., Bentsen, M., Lawrence, D.M., Lorentzen, T., Schwinger, J., Seland,

777   Ø. and Heinze, C., 2013. Evaluation of the carbon cycle components in the Norwegian Earth

778   System Model (NorESM). *Geoscientific Model Development*, *6*(2), pp.301-325.

779   Venturas, M. D., MacKinnon, E. D., Dario, H. L., Jacobsen, A. L., Pratt, R. B., & Davis, S. D.

780   (2016). Chaparral shrub hydraulic traits, size, and life history types relate to species mortality

781   during California's historic drought of 2014. PLOS One, 11(7).

782   Veblen, T.T., Kitzberger, T. and Donnegan, J., 2000. Climatic and human influences on fire

783   regimes in ponderosa pine forests in the Colorado Front Range. *Ecological applications*, *10*(4),

784   pp.1178-1195.

785   Westerling, A.L., Gershunov, A., Brown, T.J., Cayan, D.R. and Dettinger, M.D., 2003. Climate

786   and wildfire in the western United States. *Bulletin of the American Meteorological Society*,

787   *84*(5), pp.595-604.

788   Westerling, A.L., Hidalgo, H.G., Cayan, D.R. and Swetnam, T.W., 2006. Warming and earlier

789   spring increase western US forest wildfire activity. *science*, *313*(5789), pp.940-943.

790   Williams, A.P., Abatzoglou, J.T., Gershunov, A., Guzman-Morales, J., Bishop, D.A., Balch, J.K.

791   and Lettenmaier, D.P., 2019. Observed impacts of anthropogenic climate change on wildfire in

792   California. *Earth's Future*, *7*(8), pp.892-910.

793   Wullschleger, S.D., Gunderson, C.A., Hanson, P.J., Wilson, K.B. and Norby, R.J., 2002.

794   Sensitivity of stomatal and canopy conductance to elevated CO_2 concentration–interacting

795   variables and perspectives of scale. *New Phytologist*, *153*(3), pp.485-496.

796   Wu, J., Serbin, S.P., Ely, K.S., Wolfe, B.T., Dickman, L.T., Grossiord, C., Michaletz, S.T.,

797   Collins, A.D., Detto, M., McDowell, N.G. and Wright, S.J., 2020. The response of stomatal

798   conductance to seasonal drought in tropical forests. *Global Change Biology*, *26*(2), pp.823-839.

799   Wei, L., Xu, C., Jansen, S., Zhou, H., Christoffersen, B.O., Pockman, W.T., Middleton, R.S.,

800   Marshall, J.D. and McDowell, N.G., 2019. A heuristic classification of woody plants based on

801   contrasting shade and drought strategies. *Tree physiology*, *39*(5), pp.767-781.

802   Xu, C., McDowell, N.G., Sevanto, S. and Fisher, R.A., 2013. Our limited ability to predict

803   vegetation dynamics under water stress. *New Phytologist*, *200*(2), pp.298-300.

804   Xu, X., Medvigy, D., Powers, J.S., Becknell, J.M. and Guan, K., 2016. Diversity in plant

805   hydraulic traits explains seasonal and inter-annual variations of vegetation dynamics in

806   seasonally dry tropical forests. *New Phytologist*, *212*(1), pp.80-95.

807   Xu, C., McDowell, N.G., Fisher, R.A., Wei, L., Sevanto, S., Christoffersen, B.O., Weng, E. and

808   Middleton, R.S., 2019. Increasing impacts of extreme droughts on vegetation productivity under

809   climate change. *Nature Climate Change*, *9*(12), pp.948-953.

810   Yebra, M., Chuvieco, E. and Riaño, D., 2008. Estimation of live fuel moisture content from

811   MODIS images for fire risk assessment. *Agricultural and forest meteorology*, *148*(4), pp.523-

812   536.

813   Yebra, M., Dennison, P.E., Chuvieco, E., Riano, D., Zylstra, P., Hunt Jr, E.R., Danson, F.M., Qi,

814   Y. and Jurdao, S., 2013. A global review of remote sensing of live fuel moisture content for fire

815   danger assessment: Moving towards operational products. *Remote Sensing of Environment*, *136*,

816   pp.455-468.

817   Yebra, M., Quan, X., Riaño, D., Larraondo, P.R., van Dijk, A.I. and Cary, G.J., 2018. A fuel

818   moisture content and flammability monitoring methodology for continental Australia based on

819   optical remote sensing. *Remote Sensing of Environment*, *212*, pp.260-272.

820   Zarco-Tejada, P.J., Rueda, C.A. and Ustin, S.L., 2003. Water content estimation in vegetation

821   with MODIS reflectance data and model inversion methods. *Remote Sensing of Environment*,

822   *85*(1), pp.109-124.

823   Zhao, T. and Dai, A., 2015. The magnitude and causes of global drought changes in the twenty-

824   first century under a low–moderate emissions scenario. *Journal of climate*, *28*(11), pp.4490-

825   4512.

826

827

828

829

830

831
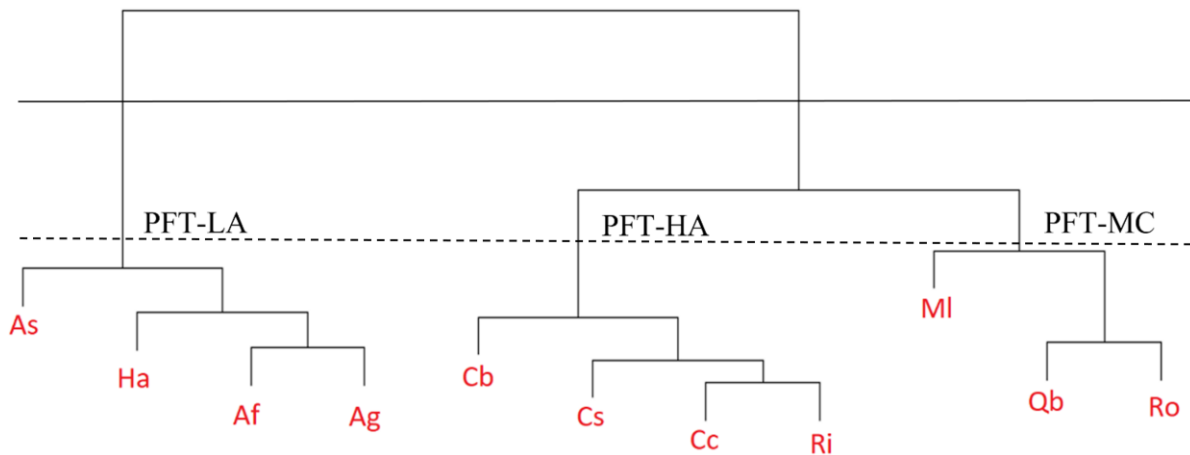
Fig 1. Hierarchical cluster analysis of allometry and hydraulic traits for eleven chaparral shrub species used to define three plant functional types at Stunt Ranch. The plant functional types with a low productivity and an aggressive drought tolerance hydraulic strategy (PFT-LA) was defined based on traits of red shank (Adenostoma sparsifolium - As), toyon (Heteromeles arbutifolia - Ha), ~~Chamise~~ chamise (Adenostoma fasciculatum - Af), big berry manzanita (Arctostaphylos glauca - Ag); the plant functional types with a high productivity and an aggressive drought tolerance hydraulic strategy (PFT-HA) was defined based on traits of mountain mahogany (Cercocarpus betuloides - Cb), greenbark ceanothus (Ceanothus spinosus - Cs), buck brush (Ceanothus cuneatus - Cc), hollyleaf redberry (Rhamnus ilicifolia - Ri); the plant functional types with a medium productivity and an conservative drought tolerance hydraulic strategy (PFT-MC) was defined based on traits of laurel sumac (Malosma laurina - Ml), scrub oak (Quercus berberidifolia - Qb), sugar bush (Rhus ovata - Ro).

844

845
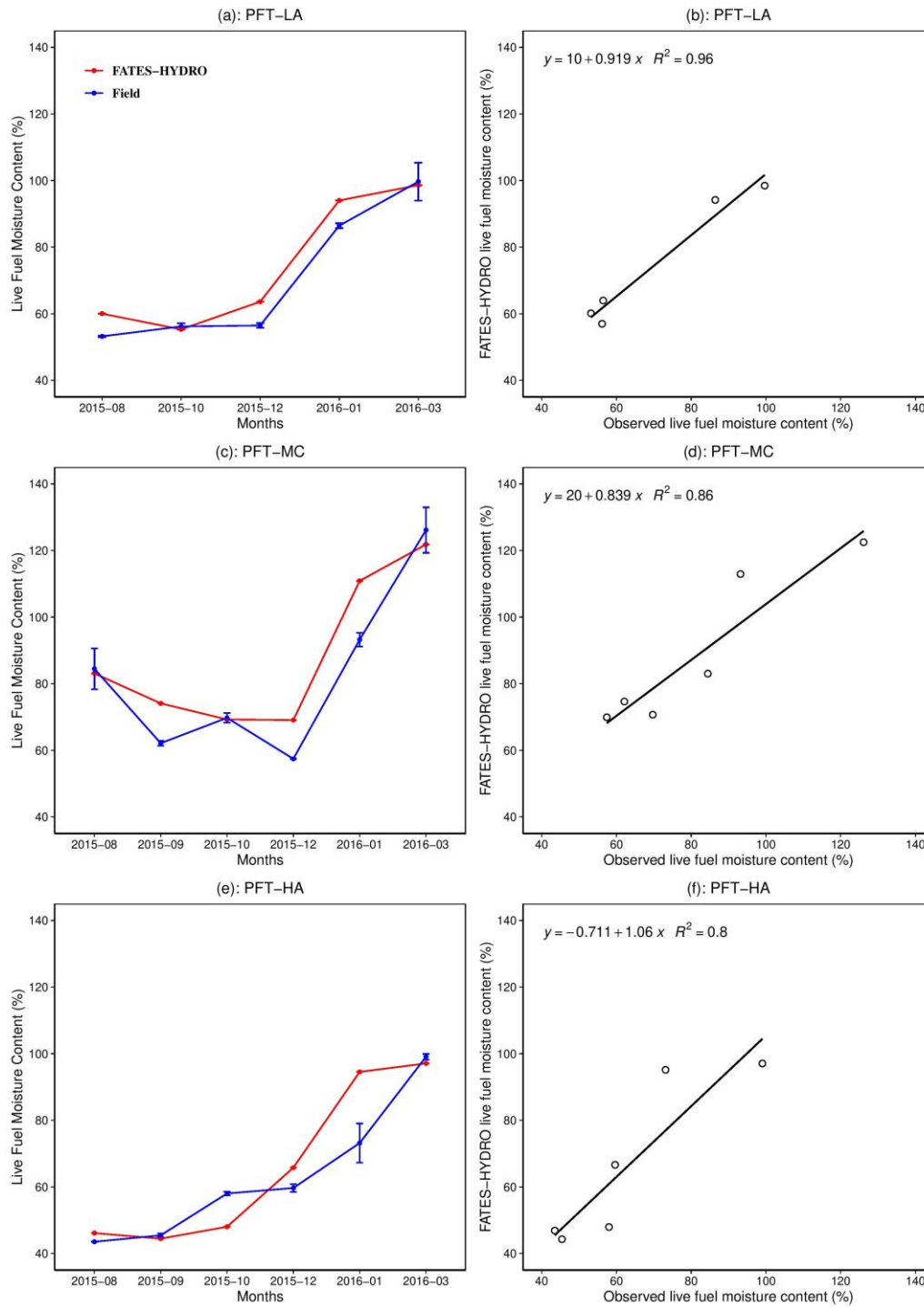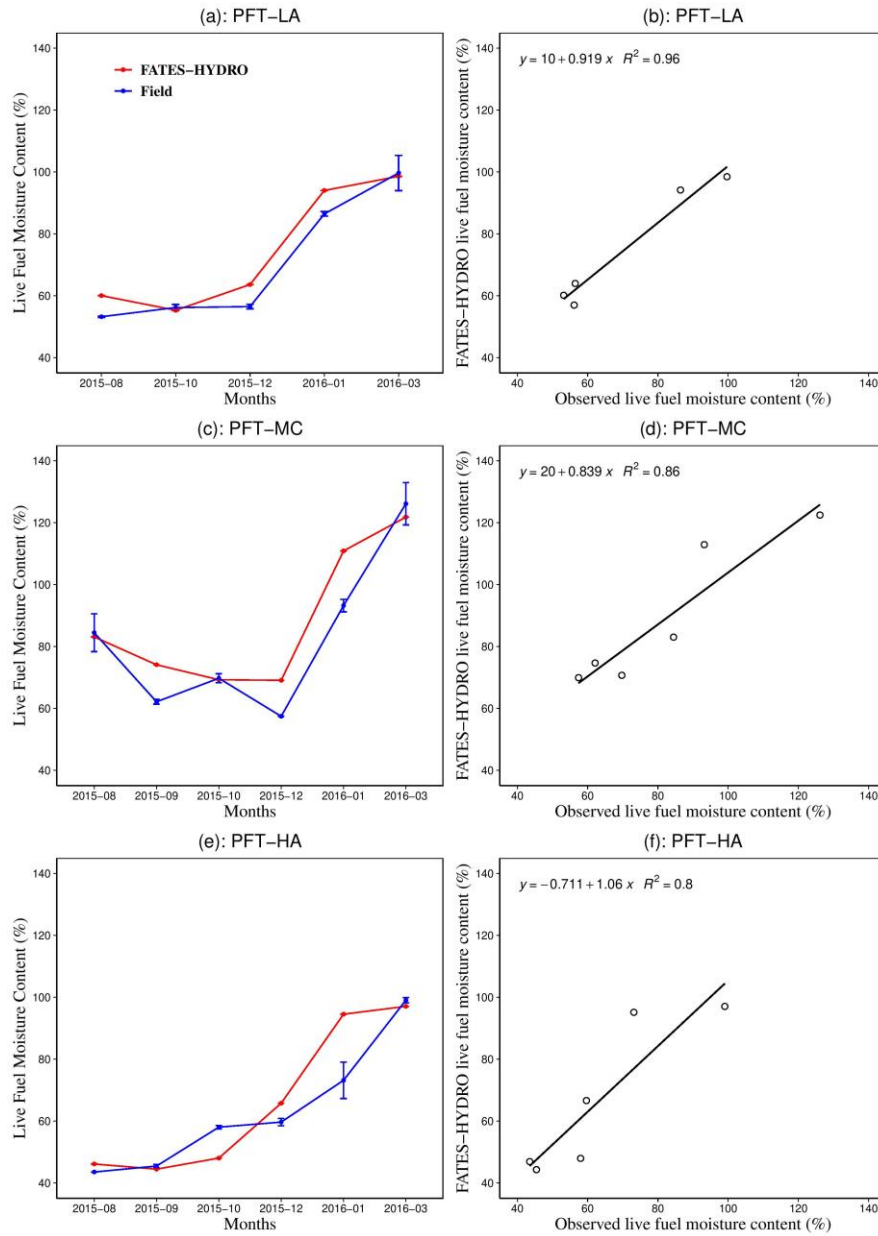
Fig.2 Simulated and observed monthly live fuel moisture content and related R^2 values for three PFTs (refer to Figure 1 for explanation of the PFTs).

848

849
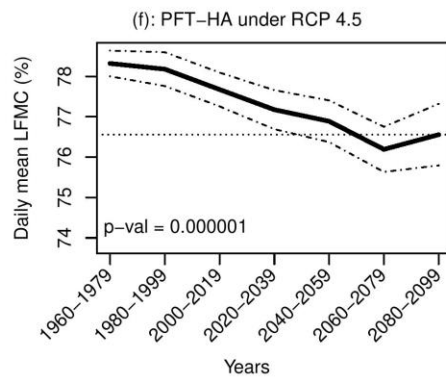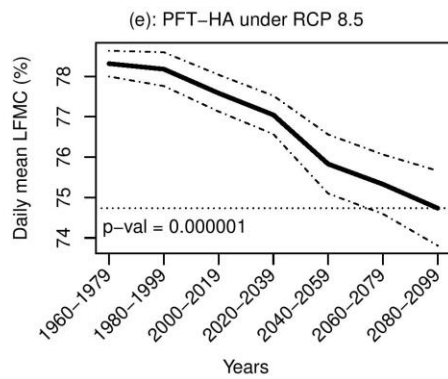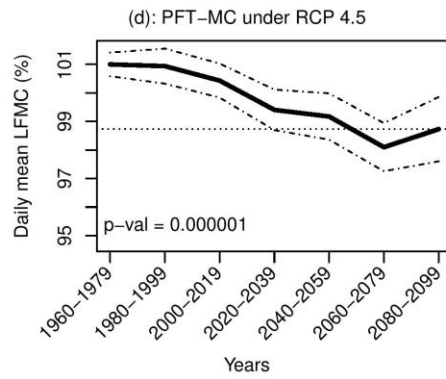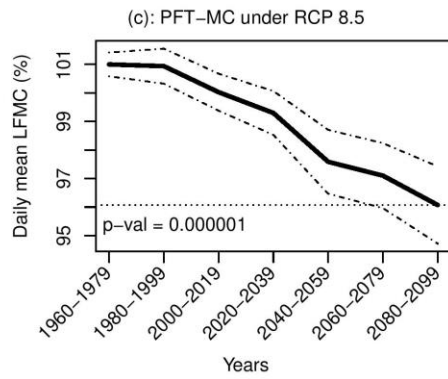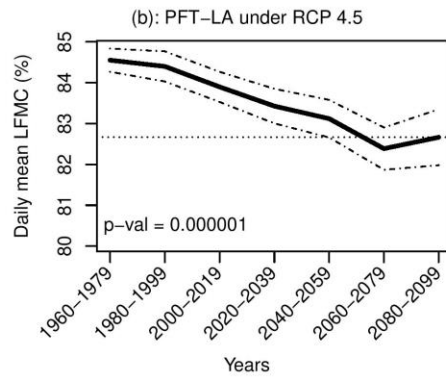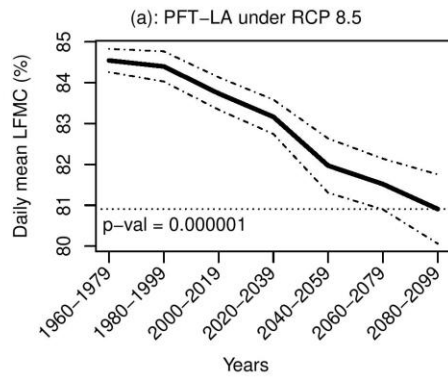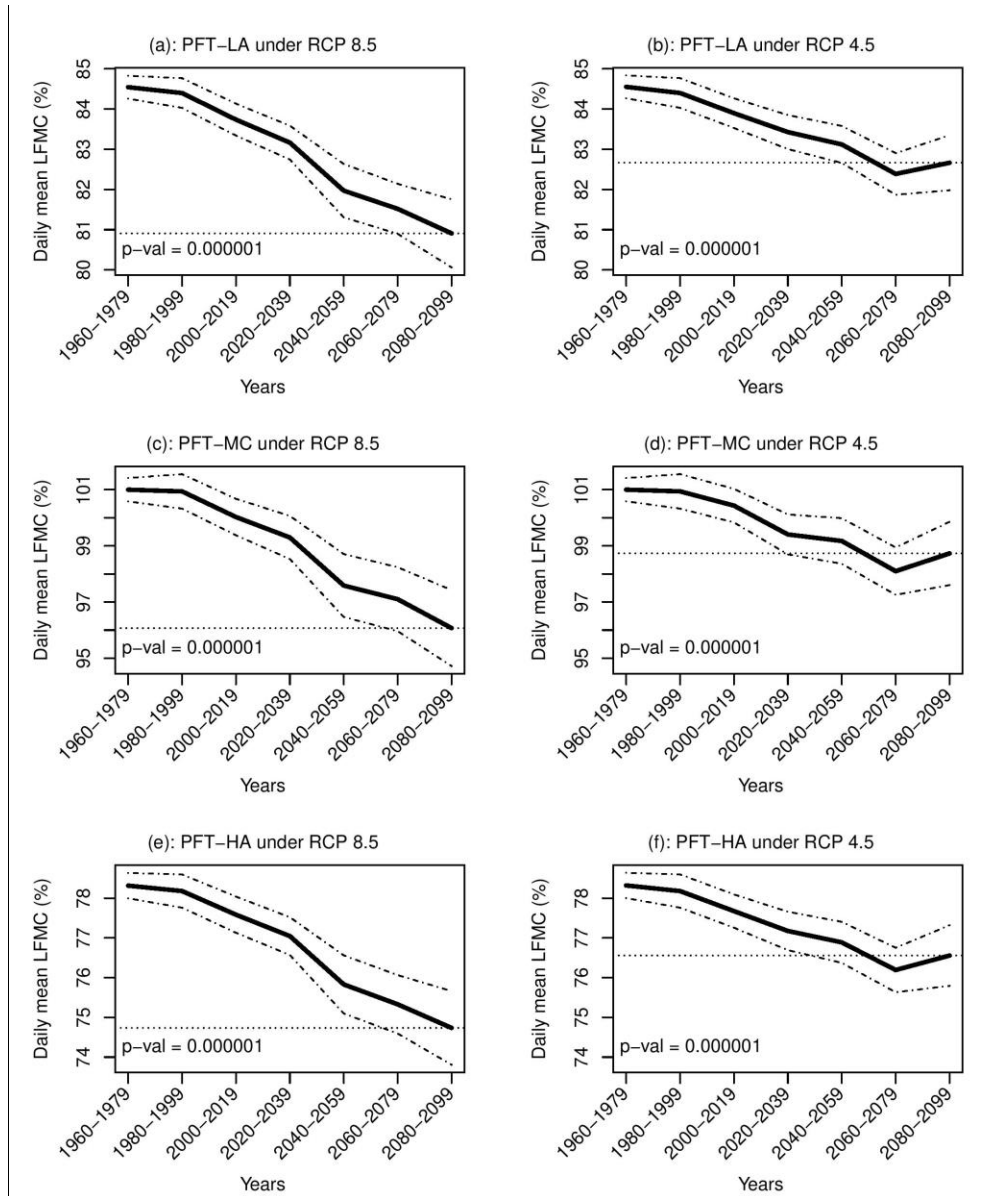
Fig.3 Temporal changes in daily mean live fuel moisture content (black solid line) and 95%
confidence interval (black dash-dot line) from 1960 to 2099 for three PFTs (refer to Figure 1 for
explanation of the PFTs) under climate scenario RCP 4.5 and 8.5 with 20 Earth System Models
considering all climatic variables changes. The P values were calculated using bootstrap
sampling to test whether the daily mean live fuel moisture content across different models during
the future period (2080–2099) was significantly lower than that during the historical period
(1960-1999). The grey horizontal dotted line represents the ensemble mean for 2080–2099.

857

858
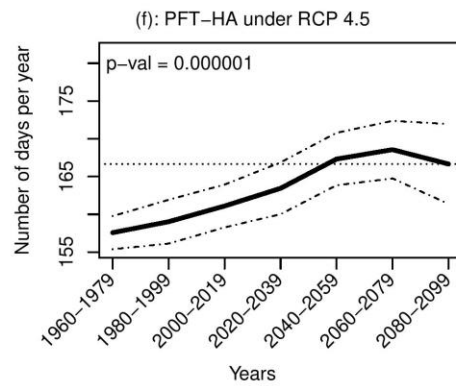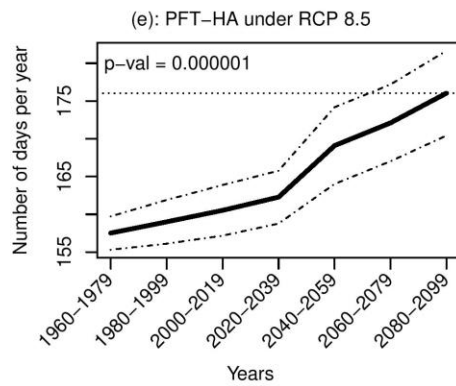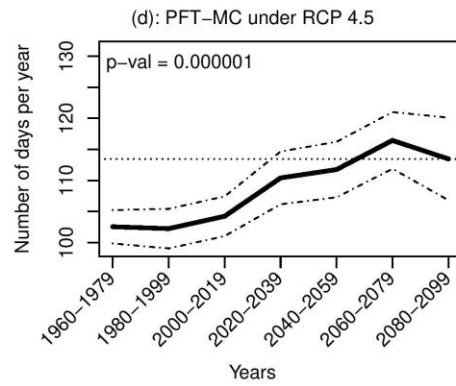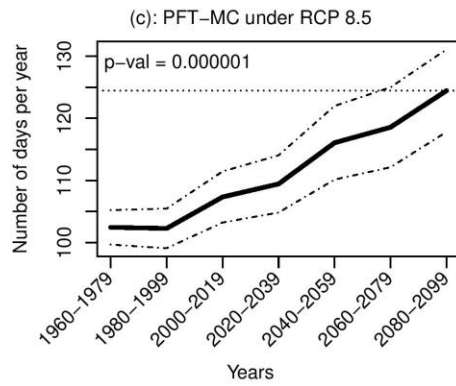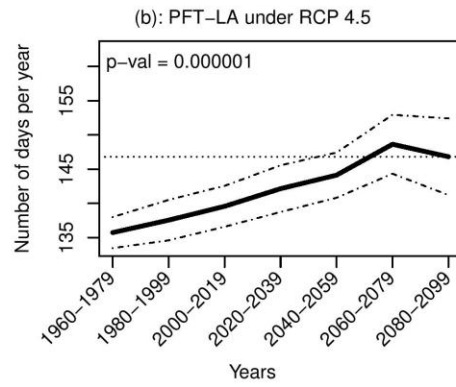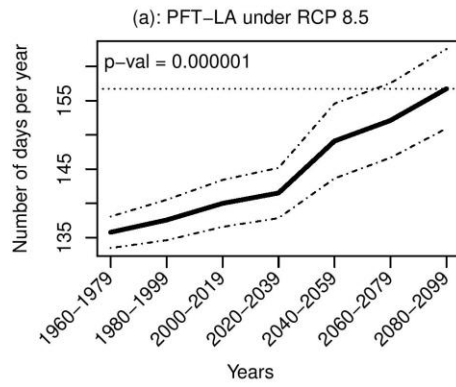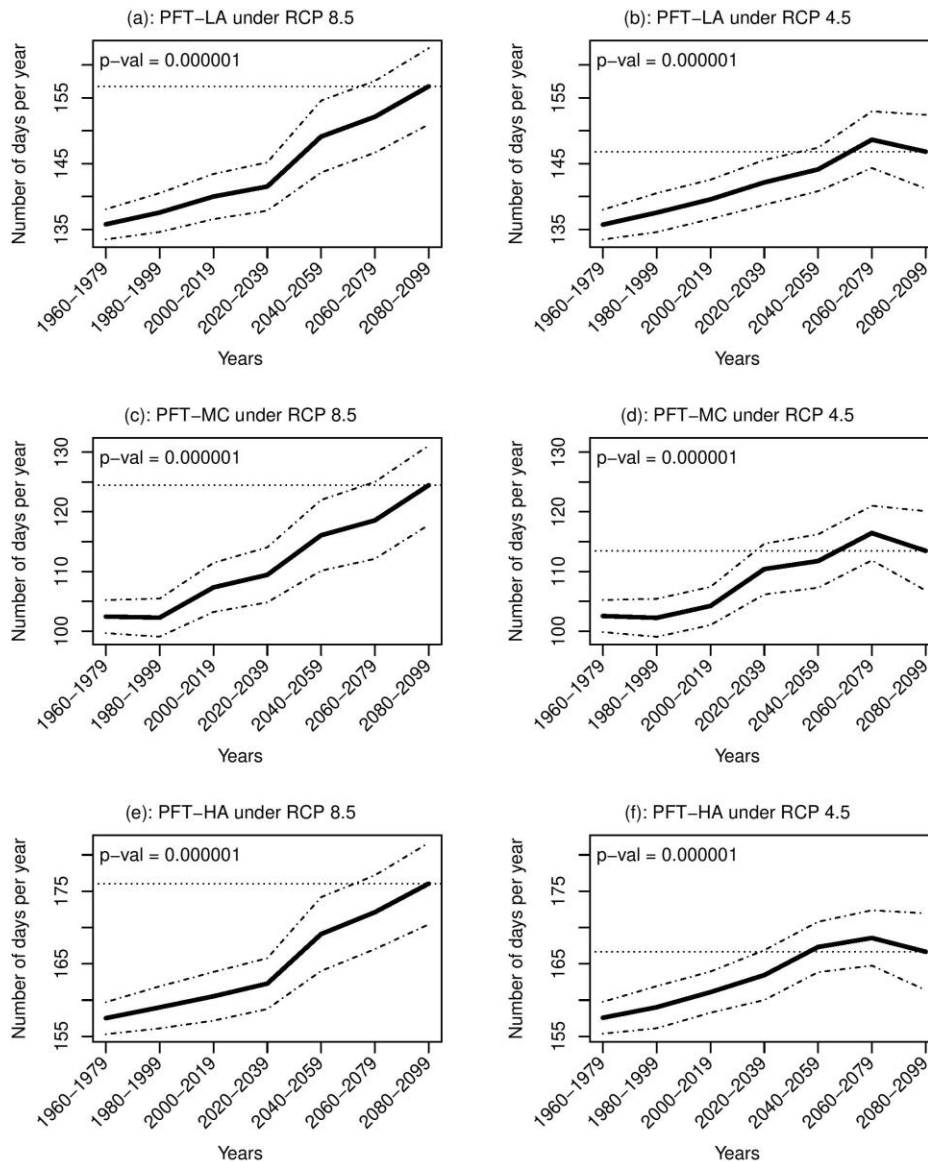
Fig.4 Temporal changes in average number of days per year of live fuel moisture content below
79% (black solid line) and 95% confidence interval (black dash-dot line) from 1960 to 2099 for
three PFTs (refer to Figure 1 for explanation of the PFTs) under climate scenario RCP 4.5 and
8.5 with 20 Earth System Models considering all climatic variables changes. The P values were
calculated using bootstrap sampling to test whether the number of days across different models
during the future period (2080–2099) was significantly higher than that during the historical
period (1960-1999). The grey horizontal dotted line represents the ensemble mean for 2080–
2099.

868

869
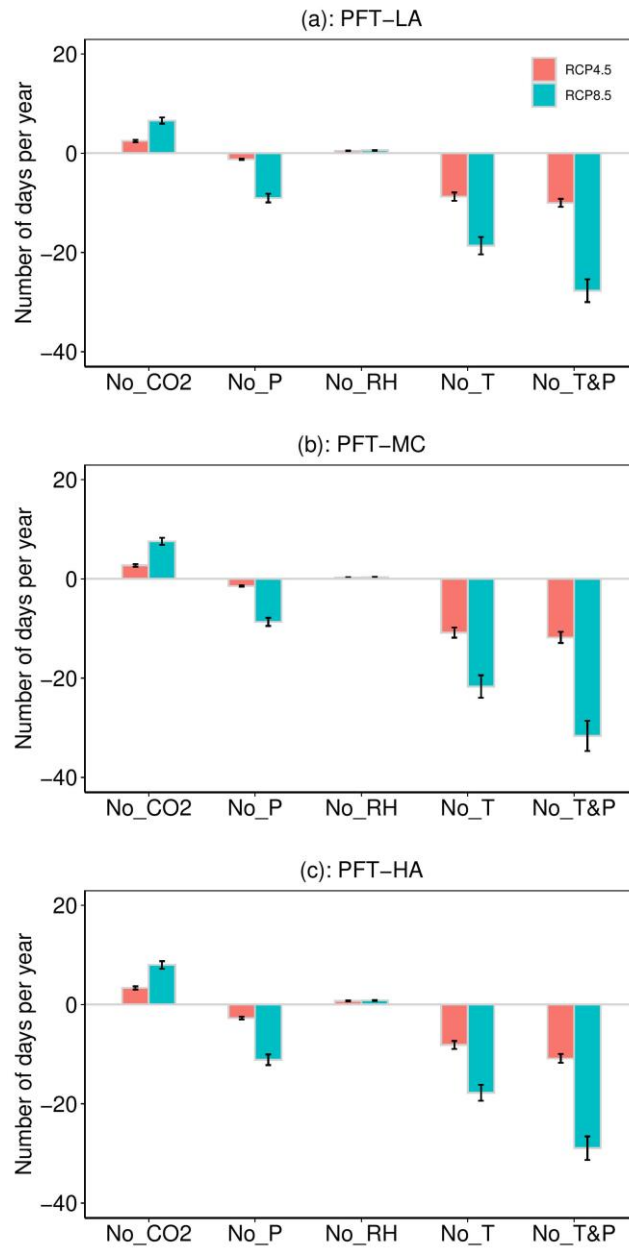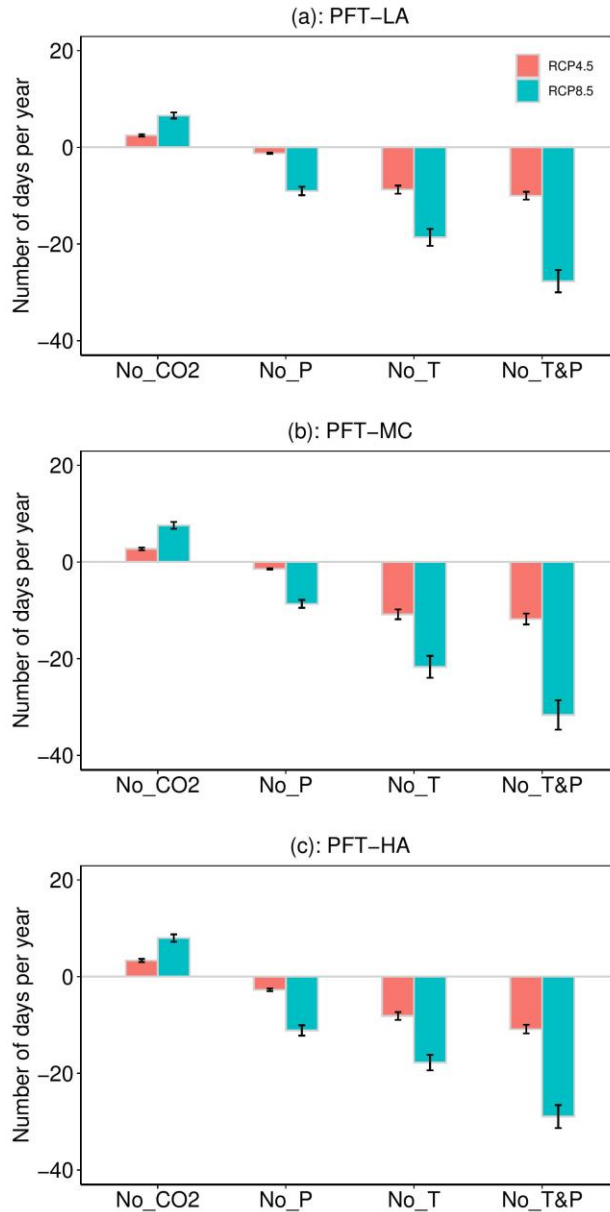
Fig.5 Differences on number of days per year of live fuel moisture content below 79% from 2080 to 2099 for three PFTs (refer to Figure 1 for explanation of the PFTs) under climate scenario RCP 4.5 and 8.5 between considering all climatic variables changes and without considering CO_2, precipitation, temperature, and precipitation & temperature~~, relative humidity~~ changes.